

VLM-CAD: VLM-Optimized Collaborative Agent Design Workflow for Analog Circuit Sizing

1st Guanyuan Pan

Hangzhou Dianzi University

Hangzhou, China

guanyuanpeterpan@gmail.com

2nd Shuai Wang*

Hangzhou Dianzi University

Hangzhou, China

shuaiwang.tai@gmail.com

3rd Yugui Lin

SCBC, GDUFS

Guangzhou, China

yuguilin0209@163.com

4th Tiansheng Zhou

Hangzhou Dianzi University

Hangzhou, China

zhoutiansheng_2024@163.com

5th Pietro Liò

University of Cambridge

Cambridge, United Kingdom

pl219@cam.ac.uk

6th Yaqi Wang*

Hangzhou Dianzi University

Hangzhou, China

wangyaqi@hdu.edu.cn

7th Zhenxin Zhao*

Hangzhou Dianzi University

Hangzhou, China

zxzhao@hdu.edu.cn

Abstract—Analog mixed-signal circuit sizing involves complex trade-offs within high-dimensional design spaces. Existing automatic analog circuit sizing approaches rely solely on netlists, ignoring the circuit schematic, which hinders the cognitive link between the schematic and its performance. Furthermore, the black-box nature of machine learning methods and hallucination risks in large language models fail to provide the necessary ground-truth explainability required for industrial sign-off. To address these challenges, we propose a Vision Language Model-optimized collaborative agent design workflow (VLM-CAD), which analyzes circuits, optimizes DC operating points, performs inference-based sizing, and executes external sizing optimization. We integrate Image2Net to annotate circuit schematics and generate a structured JSON description for precise interpretation by Vision Language Models. Furthermore, we propose an Explainable Trust Region Bayesian Optimization method (ExTuRBO) that employs collaborative warm-start from agent-generated seeds and offers dual-granularity sensitivity analysis for external sizing optimization, supporting a comprehensive final design report. Experiment results on amplifier sizing tasks using 180nm, 90nm, and 45nm Predictive Technology Models demonstrate that VLM-CAD effectively balances power and performance while maintaining physics-based explainability. VLM-CAD meets all specification requirements while maintaining low power consumption in optimizing an amplifier with a complementary input and a class-AB output stage, with a total runtime under 66 minutes across all experiments on two amplifiers.

Index Terms—Analog Circuit Sizing, Agentic AI, Vision Language Model, Explainability, Electronic Design Automation

I. INTRODUCTION

Analog and mixed-signal (AMS) integrated circuits are essential components in electronic systems [1]. However,

designing AMS circuits is complex and time-consuming. AMS circuit designers must often trade off Power, Performance, and Area to achieve balanced circuit performance, relying solely on experience. In the design process for AMS circuits, circuit sizing is particularly challenging. It involves an iterative process that balances competing objectives across various requirements, all within a high-dimensional design space. As a result, automatic circuit sizing has attracted significant research interest due to its ability to rapidly explore a wide range of design variables to identify optimal size combinations.

The evolution of automatic analog circuit sizing approaches has seen significant advancements over the years. Early efforts included Machine Learning (ML) methods [2], [3] such as Bayesian Optimization (BO) [4], [5], and Reinforcement Learning (RL) has also shown promise [6].

Language models, including Large Language Models (LLMs) and Vision Language Models (VLMs), have recently demonstrated exceptional capabilities across a range of tasks, such as code generation and multimodal reasoning. These models could propose circuit optimization strategies and analyze simulation data [7], [8]. To integrate language models with external tools, agentic workflows are becoming increasingly prominent, with engineers applying them to various tasks including automatic analog circuit sizing [9], [10].

However, current automatic analog circuit sizing approaches have the following challenges:

- **Circuit schematic underutilization:** Analog circuit schematics are vital for analog circuit designers to understand the structures and functions of transistor-level circuit netlists [11]. However, to our knowledge, no automatic analog circuit sizing approaches leverage schematics for circuit analysis or parameter optimization, relying solely on netlists. Therefore, they do not recognize the

*Corresponding Authors.

This research was supported by National Natural Science Foundation of China under Grant No. 62571173, Zhejiang Provincial Natural Science Foundation of China under Grant No. LD25F020005 and No. LQN25F030009.

spatial relationships and functional blocks visually represented in the schematic and lack the global topological context needed to make intuitive sizing decisions, leading to inefficient exploration.

- **Nonexistent or hallucinated explainability:** Industrial sign-off requires rigorous justification for every transistor size. However, ML methods often function as black boxes, delivering solutions with no insights into their internal workings. While using language models for automatic analog circuit sizing offers some level of explainability [10], this is questionable due to their tendency to hallucinate [12]. Without a quantified sensitivity analysis that clarifies the relationships between parameters and performance, automatic analog circuit sizing methods remain experimental curiosities rather than practical tools for production.

To overcome these challenges,

- 1) We propose **VLM-CAD**, a VLM-optimized collaborative agent design workflow for analog circuit sizing.
- 2) We introduce circuit schematics as inputs for automatic circuit sizing. Specifically, we use Image2Net to annotate schematics and extract component information and connections, which assist VLM in interpreting them.
- 3) We propose **ExTuRBO**, an Explainable Trust Region Bayesian Optimization method that collaboratively warm-starts local search to accelerate convergence and utilizes Automatic Relevance Determination (ARD) lengthscales to support a dual-granularity sensitivity report.

We demonstrate VLM-CAD in Fig. 1 and compare it with other state-of-the-art (SOTA) methods in TABLE I. We apply VLM-CAD to two distinct circuits using Predictive Technology Model (PTM) nodes to optimize six performance metrics [13]. The first circuit is an amplifier with a complementary input and a class-AB output stage, which we test for both 180nm and 90nm processes. The second circuit is a two-stage Miller operational amplifier at 45nm. For each circuit, VLM-CAD achieves excellent or satisfactory results.

II. RELATED WORK

A. Machine Learning and Reinforcement Learning Methods

ML techniques have shown their potential in automatic analog circuit sizing [2], [3]. BO treats transistor sizing as an optimization problem, with the objective function evaluated via simulation. RL further enhances sizing efficiency by leveraging rewards from iterative simulations, enabling better adaptation to complex design spaces [6]. However, these methods have high computational costs and inconsistent performance across different circuit designs and performance metrics [2], [4]. Additionally, their lack of explainability poses a significant barrier to their adoption in the industry, as designers are often suspicious of solutions they cannot interpret [3].

B. LLM-based Methods and Agentic Workflows

Recently, LLMs have demonstrated their capabilities to optimize analog circuits. LEDRO [7] utilized LLMs alongside

optimization techniques to iteratively refine the design space for analog circuit sizing. LLMACD [8] utilized a refined prompt manager to extract circuit representation, embed circuit knowledge, and model the knowledge-intensive design process within a Chain-of-Thought workflow. Nevertheless, LLMs have a limited understanding of AMS circuit topologies [14], making it challenging to capture the trade-offs that affect circuit performance. Additionally, their lack of mathematical precision undermines the reliability of sizing and performance estimation, underscoring the need for seamless integration with external tools, such as simulators [15].

To address these challenges in analog design, agentic workflows are becoming more prominent. AmpAgent [9] efficiently designs multi-stage amplifiers from essays using three LLM-based agents to handle process and specifications. AnaFlow [10] replicates the workflow of expert designers by introducing a multi-agent LLM workflow that provides structured reasoning and explainability in the process.

However, current SOTA LLM-based and agentic methods have limitations in their input modality, topology awareness, explainability, and initialization strategy, which we demonstrate in TABLE I.

C. Circuit Schematics and VLM

Circuit schematics are a core element of analog circuit design, as they contain information about circuit components and their connections. Schematics visually depict the structure and interconnections of a circuit, providing designers with an intuitive reference for understanding how it operates [11]. However, existing schematic resources are underutilized and have not been accurately transformed into suitable structured information for circuit simulation.

VLMs have the potential to understand circuit schematics, offering unique advantages for handling legacy design documents and generating layouts, thereby garnering attention in the field. MAPS [16] finetunes a VLM to convert pixel-level circuit schematics into SPICE netlists, offering an end-to-end path from images to simulatable netlists. CURVLM [17] applies Group Relative Policy Optimization to finetune the VLM to interpret digital circuit schematics. However, existing methods still struggle to interpret circuit schematics, demonstrating insufficient accuracy and thus are not reliable for automatic circuit sizing [18], [19].

III. VLM-CAD AGENTIC WORKFLOW

A. Image2Net Interpreting Circuit Schematic

Despite excellent performance on object detection and complex multimodal reasoning tasks, VLMs struggle to count intersections in line diagrams or identify geometric relationships among intersecting circles [18]. This limitation raises concerns about their ability to interpret schematics and understand circuit connectivity.

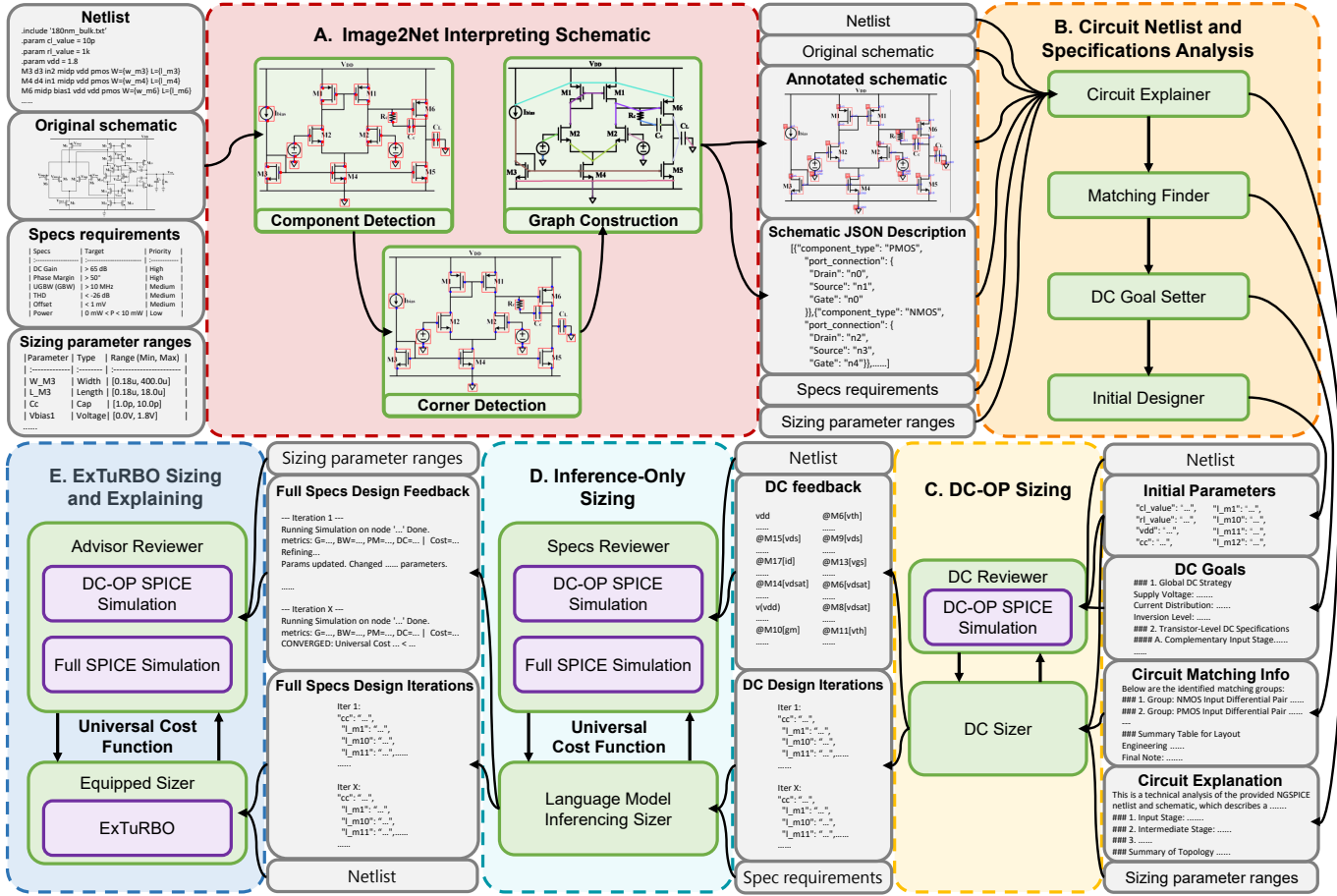


Fig. 1: VLM-CAD overview. We include five stages for VLM-CAD: A. Image2Net Interpreting Circuit Schematic (see Sec. III-A), B. Circuit Netlist and Specifications Analysis (see Sec. III-B), C. DC-OP Sizing (see Sec. III-C), D. Inference-Only Sizing (see Sec. III-D) and E. Sizing and Explaining (see Sec. III-E).

TABLE I: Comparison of VLM-CAD features with SOTA methods. VLM-CAD incorporates schematic and netlist multimodality, LLM with ARD for quantified explainability, and LLM with ExTuRBO for Collaborative Warm-Start initialization strategy.

Framework	Input Modality	Topology Awareness	Explainability	Initialization Strategy
LLMACD [8]	Netlist (Text)	Netlist Inference	LLM CoT (Hallucinated)	LLM
AmpAgent [9]	Literature + Netlist (Text)	Formula-based	LLM ReAct (Hallucinated)	LLM + Black-box Optimizer
AnaFlow [10]	Netlist (Text)	Netlist Inference	LLM (Hallucinated)	LLM + Black-box Optimizer
VLM-CAD (Ours)	Schematic + Netlist (Multimodal)	Schematic + Netlist Inference	LLM + ARD (Quantified)	LLM + ExTuRBO (Collaborative Warm-Start)

We therefore utilize Image2Net¹, a hybrid framework combining DL-based object detection with heuristic computer vision algorithms to annotate the schematic and extract information about components and their connections.

- Component Detection:** We employ a finetuned YOLOv8-Pose model to identify the bounding boxes of components and predict the coordinates of terminal poses. We then align these coordinates with the nearest wire pixels to ensure accurate anchoring.
- Corner Detection:** To effectively capture the wiring topology, we apply a combination of feature detection

¹Image2Net was proposed by Yiren Pan (panyiren@hdu.edu.cn) and won the first prize of the 2024 China Postgraduate IC Innovation Competition - EDA Elite Challenge Contest.

algorithms, including Harris, Shi-Tomasi, Oriented FAST and Rotated BRIEF, Scale-Invariant Feature Transform, and Binary Robust Invariant Scalable Keypoints, to maximize corner detection recall. We then employ Density-Based Spatial Clustering of Applications with Noise clustering to merge any duplicate detections.

- Graph Construction:** Next, we create a connectivity graph by verifying pixel-level continuity between component pins and corners in the binarized schematic. We verify this using a hybrid approach: we employ efficient vectorized array slicing to validate orthogonal connections, and Bresenham's algorithm to trace diagonal paths. We then aggregate the validated segments to form graph edges, clustering all physically connected nodes

into distinct electrical nets.

- **Annotated Schematic and JSON Description Generation:** Finally, we parse the resulting graph to map component ports to net identifiers, generating a JSON description of the schematic that includes its components and their connections. Additionally, we create an annotated schematic that color-codes the distinct electrical connections for verification.

We present the details of this phase in Fig. 1.A.

B. Circuit Netlist and Specifications Analysis

After annotating the schematic and extracting information about components and their connections, we conduct a deep analysis of the analog circuit sizing problem using a sequence of specialist agents, thereby decomposing the complex task.

- **Circuit Explainer:** This VLM Agent serves as the cognitive foundation of the workflow. It ingests both the circuit schematic images and the SPICE netlist, along with performance specifications. Beyond basic connectivity analysis, it leverages visual and textual data to identify analog sub-blocks, such as differential pairs and current mirrors, deduce signal flow and feedback mechanisms, and synthesize a holistic understanding of the circuit’s operation. This high-level analysis provides the necessary context for all subsequent sizing and optimization agents.
- **Matching Finder:** Leveraging both the schematic and the netlist, this VLM agent identifies transistor clusters that require precise symmetry. Notably, it goes beyond simple grouping by explicitly defining parameter-level constraints for each group. It also infers layout implications, for instance, needs for interdigitation, and provides the engineering rationale for these constraints, ensuring the subsequent sizing process respects the physical layout of the device matching.
- **DC Goal Setter:** Acting as the biasing strategist, this agent translates the topology into quantitative DC operating targets. Instead of generic operating regions, it defines specific targets for Overdrive Voltage, Drain-Source Voltage, and Current Density for every transistor. It creates a global bias distribution plan, ensuring sufficient voltage headroom for signal swing and defining the necessary start-up conditions for the circuit to converge.
- **Initial Designer:** This agent generates the complete initial parameter set required to start the simulation. To guarantee executability, the workflow employs a dynamic Prompt Injection technique: it parses the raw netlist to extract all mandatory variables and forces the agent to populate exactly those keys, preventing parameter hallucination or omission. The agent prioritizes simulability and convergence by selecting conservative, stable values aligned with the DC goals, ensuring the design serves as a valid starting point for subsequent numerical phases.

We present the details of this phase in Fig. 1.B.

C. DC-OP Sizing

With previous analysis results, VLM-CAD initiates a preparatory second phase to establish a reasonable DC-biased solution before conducting costly performance simulations. During this phase, the goal is not to achieve perfect DC convergence, but to quickly gain insights into the circuit’s behavior in the target technology using limited language model calls and simulations.

- **DC Reviewer:** This agent serves as the validation gate-keeper, orchestrating a fast DC operating point SPICE simulation focusing on the target output node DC level to ensure proper biasing. It extracts node voltages and device operating points and compares these against the DC goals from previous analysis, generating a structured discrepancy report that quantifies headroom violations and region errors. It calculates a discrepancy count that serves as the stopping criterion for the optimization loop.
- **DC Sizer:** This agent executes the inferencing-based parameter refinement. It ingests the discrepancy report and applies analog design heuristics to resolve biasing issues. Notably, we enforce full-set consistency here to ensure that static testbench parameters, matching constraints and physical range limits are strictly preserved across iterations, preventing simulation divergence.

We present the details of this phase in Fig. 1.C.

D. Inference-Only Sizing

After refining the DC-OP sizing, we proceed to optimize all the necessary specifications through full simulations. During this phase, VLM-CAD relies exclusively on the inherent knowledge of analog circuit theory provided by language models, along with context from previous agents, to enhance the design without any external numerical optimizers. With sample-efficient loops, this phase aims to swiftly find optimal designs before resorting to simulation-intensive optimizers.

To transform the multi-objective analog circuit sizing task into a scalar optimization task suitable for both the language model agents and the numerical optimizer, we define a **Universal Cost Function**, denoted as $J(\mathbf{x})$, to guide the search through two distinct phases: **Feasibility** and **Optimization**. The Feasibility phase aims to satisfy all specifications except for power, while the Optimization phase focuses on minimizing power consumption. For a given set of design parameters \mathbf{x} , we define the Universal Cost Function $J(\mathbf{x})$ as follows:

$$J(\mathbf{x}) = \frac{P_{\text{meas}}(\mathbf{x})}{P_{\text{max}}} + \sum_{i \in \mathcal{S}} w_i \cdot \mathcal{V}_i(y_i(\mathbf{x}), T_i) + \mathcal{P}_{\text{sanity}}. \quad (1)$$

Here:

- P_{meas} is the simulated power consumption and P_{max} is the maximum allowable power specification.
- \mathcal{S} represents the set of all performance metrics. We divide this set into lower-bound specifications \mathcal{S}_{LB} , such as gain and PM, and upper-bound specifications \mathcal{S}_{UB} , such as THD and offset.

- w_i represents the penalty weight for metric i , prioritizing critical specs.
- \mathcal{V}_i is the Rectified Linear Unit (ReLU) violation function. We define \mathcal{V}_i as follows to handle the directionality of different specifications rigorously:

$$\mathcal{V}_i(y_i(\mathbf{x}), T_i) = \begin{cases} \max(0, T_i - y_i(\mathbf{x})), & i \in \mathcal{S}_{LB} \\ \max(0, y_i(\mathbf{x}) - T_i), & i \in \mathcal{S}_{UB}. \end{cases} \quad (2)$$

- $\mathcal{P}_{\text{sanity}}$ is a significant constant penalty applied only when fundamental functionality is compromised, such as non-convergence or near-zero gain, serving as a soft barrier to guide the search away from non-functional areas.

This formulation creates a smooth optimization landscape: when $J(\mathbf{x}) > 1$, the agents focus on satisfying all specifications except for power (Feasibility Mode). Once $J(\mathbf{x}) \leq 1$, the logic naturally transitions to minimizing power while maintaining compliance (Optimization Mode).

We present the details of this phase in Fig. 1.D:

- **Specs Reviewer:** This agent functions as a rigorous validation engine, using a hybrid DC/AC simulation strategy combined with a Skip-on-Fail mechanism to evaluate design performance efficiently. Instead of performing computationally expensive simulations indiscriminately, it first verifies the DC operating point. If the circuit fails basic biasing checks, the process is halted early to conserve resources. Once the simulation is successful, it computes $J(\mathbf{x})$ via (1), which quantifies the design's compliance with the specifications and serves to assess the optimization status.
- **Language Model Inferencing Sizer:** This agent performs parameter refinement based on inferencing, utilizing a history-aware context window to avoid optimization oscillation. Guided by $J(\mathbf{x})$ (1), it dynamically alternates between strategies for satisfying constraints and minimizing power consumption. To ensure robustness against stagnation, the workflow includes a dead loop detection and perturbation mechanism: if the agent suggests a parameter set identical to the previous iteration, the system automatically applies a 5% random perturbation to transistor widths, which disrupts the inferencing deadlock and propels the simulator into a new state, enabling the optimization process to regain momentum.

E. ExTuRBO Sizing and Explaining

When inference-only sizing reaches its iteration limit or convergence plateau, we escalate to the final optimization stage, where VLM-CAD transitions from qualitative inferencing to quantitative precision.

We propose **ExTuRBO**, an Explainable Trust Region Bayesian Optimization method to bridge the gap between language models and black-box optimization. Unlike standard Trust Region Bayesian Optimization (TuRBO), we design ExTuRBO with two unique features:

- **Collaborative Warm-Start:** TuRBO initializes with a Latin Hypercube Sampling (LHS) of the entire high-

dimensional search space, which wastes significant simulation budget exploring non-functional regions. ExTuRBO, conversely, is seeded by the agents. We extract the unique set of high-performing candidates $\mathcal{D}_{\text{seed}}$ from the inference-only sizing phase.

The Trust Regions for the parallel independent workers are initialized centering on these seeds:

$$\mathbf{x}_{\text{center}}^{(0)} = \arg \min_{\mathbf{x} \in \mathcal{D}_{\text{seed}}} J(\mathbf{x}). \quad (3)$$

TuRBO initializes via LHS over the entire global design space $\mathcal{X}_{\text{global}} \subset \mathbb{R}^D$. Given the high dimensionality of analog sizing, the global volume V_{global} becomes prohibitively large, leading to high sample complexity when attempting to locate a feasible region. In contrast, by employing Collaborative Warm-Start, VLM-CAD effectively prunes the search space, defining a localized subspace $\mathcal{X}_{\text{local}}$ centered around the semantic seed \mathbf{x}_{seed} with a contracted span ratio $r < 1$. The reduction in search volume is exponential relative to the dimension:

$$\frac{V_{\text{local}}}{V_{\text{global}}} \approx \prod_{d=1}^D r_d \approx r^D. \quad (4)$$

For a 48-dimensional problem with $r = 0.4$, the effective search space is reduced by a factor of $\sim 10^{19}$, allowing ExTuRBO to skip the exploration phase and focus immediately on exploitation within the high-probability region identified by previous phases.

- **Dual-Granularity Explainability:** To provide ground-truth explainability required for the final design report, ExTuRBO utilizes Automatic Relevance Determination (ARD). We define the kernel function as follows:

$$k(\mathbf{x}, \mathbf{x}') = \sigma_f^2 \exp \left(- \sum_{d=1}^D \frac{(x_d - x'_d)^2}{2\ell_d^2} \right). \quad (5)$$

Here, ℓ_d is the lengthscale of parameter d . We define the Feature Importance S_d as the inverse lengthscale: $S_d \propto 1/\ell_d$, as a small ℓ_d implies high sensitivity.

ExTuRBO fits two distinct GP models post-optimization to generate insights: **Global Sensitivity**, which we fit on the entire dataset and identifies survival parameters that determine basic circuit feasibility, and **Elite Sensitivity**, which we fit only on the top 15% of designs and identifies tuning parameters that drive high-performance metrics.

We present the details of this phase in Fig. 1.E:

- **Advisor Reviewer:** This agent acts as the bridge between the inference-only sizing phase and the numerical phase. It analyzes the optimization history and filters the iteration logs to identify the best unique candidates for seeding. It then configures ExTuRBO's search bounds based on the stagnation context and explicitly triggers the external tool.
- **Equipped Sizer:** This agent serves as the execution interface for the numerical engine. It configures the parallel ExTuRBO workers with the seeds provided by

TABLE II: Sizing parameter ranges for: (a) the amplifier with a complementary input and a class-AB output stage, and (b) the two-stage Miller operational amplifier.

Parameter	PTM 180 nm	PTM 90 nm
Width (μm)	[0.18, 400]	[0.09, 400]
Length (μm)	[0.18, 18]	[0.09, 9]
Bias Voltage (V)	(0, 1.8)	(0, 1.2)
Supply Voltage (V)	1.8	1.2
Compensation Capacitor (pF)	[1, 10]	[1, 10]
Load Capacitor (pF)	10	10
Load Resistor ($\text{k}\Omega$)	1	1

(b)

Parameter	PTM 45 nm
Width (μm)	[0.25, 5]
Length (nm)	[45, 225]
Multiplier	[1, 25]
Supply Voltage (V)	1.2
Compensation Capacitor (pF)	[0.1, 10]
Load Capacitor (pF)	10
Bias Current Source (μA)	30

the Advisor. Upon completion of the numerical run, it serves as the result explainer: utilizing the lengthscales ℓ_d from (5), it incorporates insights from Global Sensitivity and Elite Sensitivity utilizing the lengthscales ℓ_d from (5), synthesizing them into a comprehensive design sign-off report that details the selected optimal parameters. Additionally, the report explains the rationale for these choices, distinguishing between parameters fixed for stability and those adjusted for enhanced performance.

IV. EXPERIMENTS

A. Experimental Setup

We utilize VLM-CAD to size two distinct circuits (see Fig. 2): 1) An amplifier with a complementary input and a class-AB output stage [20]. We size it using both the 180nm and 90nm BSIM predictive technology models [13]. 2) A two-stage Miller operational amplifier [21]. We size it using the 45nm BSIM predictive technology model [13].

We use Gemini 3 Flash Preview, GPT-5.2 and Qwen3-VL-235B-A22B-Instruct [22] as the VLMs and Ngspice for all simulations here. We consider six specification constraints for optimization: Gain, Phase Margin (PM), Unity Gain Bandwidth (UGBW), Total Harmonic Distortion (THD), Input Offset, and Power. We aim to minimize or maintain low power consumption while satisfying all other specification constraints. We define the ranges for the sizing parameters, summarized in TABLE II.

For the Universal Cost Function, we use the following metric penalty weight: $w_{gain} = 1.0$, $w_{ugbw} = 0.2$, $w_{pm} = 0.1$, $w_{thd} = 0.5$, $w_{offset} = 10.0$. We set $\mathcal{P}_{sanity} = 100.0$. In each experiment, we set the following limits: 1) Phase C has a maximum of 10 iterations to find a reasonable DC-biased solution, 2) Phase D is limited to 40 iterations until

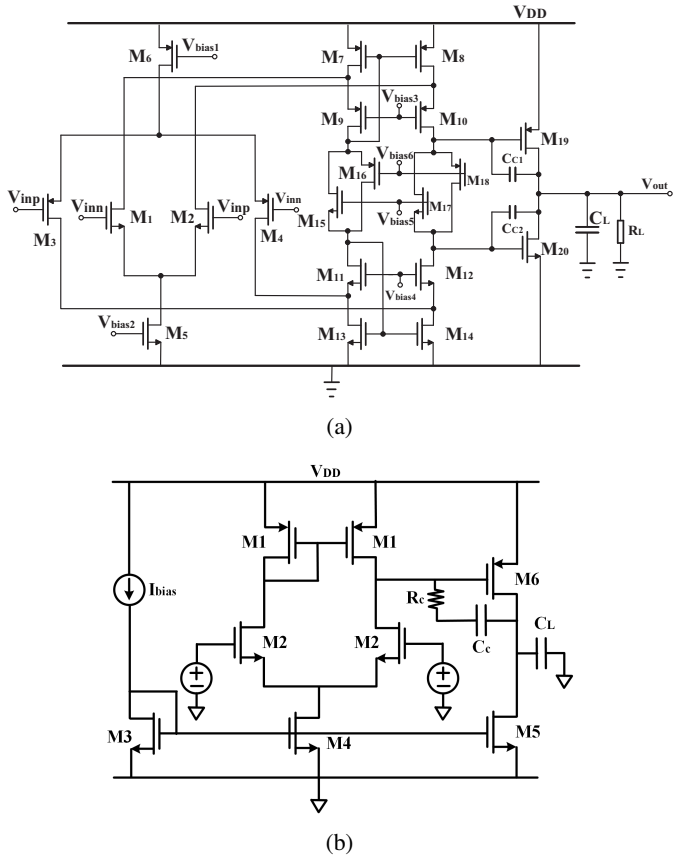


Fig. 2: Schematics of the two amplifiers we use: (a) an amplifier with complementary input and a class-AB output stage, and (b) a two-stage Miller operational amplifier.

the Universal Cost (UC) reaches 0.5, and 3) ExTuRBO of Phase E has a maximum budget of 400 iterations to achieve a universal cost of 0.5, followed by an additional 40 iterations to reduce power consumption.

B. Results and Analysis

We present the optimization results of VLM-CAD in TABLE III and the average runtime in TABLE IV. VLM-CAD successfully optimizes the amplifier with a complementary input and a class-AB output stage. It meets all specification requirements while maintains low power consumption in every attempt. For optimization of the amplifier with a complementary input and a class-AB output stage, VLM-CAD achieves a total runtime of under 9 minutes. For optimization of the two-stage Miller operational amplifier, VLM-CAD achieves a total runtime of under 66 minutes. Both sets of experiments demonstrate that VLM-CAD significantly outperforms existing approaches regarding total runtime.

Nevertheless, for the two-stage Miller operational amplifier, VLM-CAD did not consistently meet the Gain and PM specification requirements, while exceeding the allowable power consumption in some attempts. This discrepancy stems from the significantly different sizes of the feasible design spaces for the two circuits, highlighting a critical limitation of current lan-

TABLE III: Optimization results for the two amplifiers we use in our experiments. **Red** fonts denote metrics that did not meet the specification requirements.

(a) Optimization results for the amplifier with a complementary input and a class-AB output stage.

PTM	VLM	Gain (≥ 65 dB)	UGBW (≥ 10 MHz)	PM ($\geq 50^\circ$)	THD (≤ -26 dB)	Offset (≤ 1 mV)	Power (≤ 10 mW)	UC
180nm	Gemini 3 Flash Preview	85.505	35.111	51.897	-94.375	0.551	0.810	0.081
	GPT-5.2	84.684	13.647	50.853	-109.475	0.670	0.107	0.011
	Qwen3-VL-235B-A22B-Instruct	66.833	23.747	53.192	-82.220	0.869	0.357	0.036
90nm	Gemini 3 Flash Preview	71.808	32.183	52.374	-95.270	0.997	0.366	0.037
	GPT-5.2	76.521	18.526	76.825	-74.361	0.960	0.258	0.026
	Qwen3-VL-235B-A22B-Instruct	77.064	10.724	60.704	-112.792	0.950	1.090	0.109

(b) Optimization results for the two-stage Miller operational amplifier.

PTM	VLM	Gain (≥ 54 dB)	UGBW (≥ 1 MHz)	PM ($\geq 60^\circ$)	THD (≤ -60 dB)	Offset (≤ 5 mV)	Power ($45-85$ μ W)	UC
45nm	Gemini 3 Flash Preview	53.180	1.523	48.703	-77.933	3.838	68.321	2.754
	GPT-5.2	52.525	8.107	64.646	-68.949	4.417	70.040	2.299
	Qwen3-VL-235B-A22B-Instruct	53.037	30.035	11.918	-85.131	0.604	161.538	7.671

TABLE IV: Average runtime for the optimization of the two amplifiers. **Red** and **blue** fonts denote the shortest and the second shortest average runtime, respectively.

(a) Average runtime for the optimization of the amplifier with a complementary input and a class-AB output stage.

PTM	VLM	Phase B		Phase C		Phase D		Phase E		Total
		Time (s)	Iter	Time (s)	Iter	Time (s)	Seed	Time (s)	Time (s)	
180nm	Gemini 3 Flash Preview	140.3	1	7.8	2	6.1 (2.06%)	1	129.1 (43.56%)	296.4	
	GPT-5.2	271.7	1	21.8	40	222.9 (10.59%)	3	1575.3 (74.82%)	2105.4	
	Qwen3-VL-235B-A22B-Instruct	165.1	1	4.7	17	207.3 (34.32%)	3	213.3 (35.31%)	604.0	
90nm	Gemini 3 Flash Preview	81.4	1	6.3	2	26.5 (9.18%)	1	160.5 (55.59%)	288.7	
	GPT-5.2	271.1	1	29.0	1	0.6 (0.12%)	1	188.8 (37.62%)	501.9	
	Qwen3-VL-235B-A22B-Instruct	328.9	1	15.8	6	116.9 (17.51%)	1	193.0 (28.91%)	667.7	

(b) Average runtime for the optimization of the two-stage Miller operational amplifier.

PTM	VLM	Phase B		Phase C		Phase D		Phase E		Total
		Time (s)	Iter	Time (s)	Iter	Time (s)	Seed	Time (s)	Time (s)	
45nm	Gemini 3 Flash Preview	87.5	1	5.4	40	166.7 (7.17%)	3	2053.1 (88.35%)	2323.8	
	GPT-5.2	351.6	1	57.0	40	1110.2 (28.42%)	3	2377.6 (60.86%)	3906.4	
	Qwen3-VL-235B-A22B-Instruct	347.2	1	8.0	40	618.4 (19.44%)	3	2194.3 (68.98%)	3181.0	

TABLE V: Average runtime of VLM-CAD and both ablation studies. **Red** and **blue** fonts denote the shortest and the second shortest average runtime, respectively. Phase E of both ablation studies accounts for a larger portion of the total runtime than VLM-CAD's.

(a) Average runtime for the amplifier with a complementary input and a class-AB output stage.

PTM		Phase A		Phase B		Phase C		Phase D		Phase E		Total
		Time (s)	Time (s)	Time (s)	Iter	Time (s)	Iter	Time (s)	Seed	Time (s)	Time (s)	
180nm	VLM-CAD	13.58 \pm 1.38	119.26 \pm 19.93	1	6.62 \pm 0.67	13.4 \pm 1.1	91.28 \pm 106.22 (23.42%)	2.0 \pm 0.9	159.06 \pm 71.23 (40.81%)	389.80 \pm 122.28		
	Ablation 1	-	102.66 \pm 6.67	1	13.62 \pm 8.88	24.8 \pm 18.6	183.18 \pm 147.42 (12.74%)	2.4 \pm 0.8	1137.94 \pm 897.04 (79.17%)	1437.40 \pm 984.50		
	Ablation 2	-	75.48 \pm 7.14	1	9.38 \pm 3.93	13.8 \pm 13.7	88.96 \pm 108.14 (10.84%)	2.4 \pm 0.8	646.52 \pm 623.37 (78.81%)	820.34 \pm 608.73		
90nm	VLM-CAD	13.70 \pm 0.83	95.86 \pm 9.03	1	6.50 \pm 0.21	1.8 \pm 1.2	9.16 \pm 10.86 (3.48%)	1.4 \pm 0.8	138.04 \pm 16.00 (52.43%)	263.26 \pm 22.55		
	Ablation 1	-	96.60 \pm 16.39	1	6.12 \pm 0.70	2.0 \pm 1.3	178.12 \pm 8.39 (7.33%)	1.8 \pm 1.0	2150.48 \pm 1151.21 (88.45%)	2431.32 \pm 1150.02		
	Ablation 2	-	78.62 \pm 7.90	1	7.68 \pm 1.15	7.0 \pm 7.5	36.82 \pm 45.10 (12.30%)	1.8 \pm 1.0	176.30 \pm 62.86 (58.88%)	299.42 \pm 104.50		

(b) Average runtime for the two-stage Miller operational amplifier.

PTM	Run	Phase A		Phase B		Phase C		Phase D		Phase E		Total
		Time (s)	Time (s)	Time (s)	Iter	Time (s)	Iter	Time (s)	Seed	Time (s)	Time (s)	
45nm	VLM-CAD	15.38 \pm 5.19	97.04 \pm 18.25	1	19.16 \pm 24.36	40.0 \pm 0.0	180.02 \pm 11.17 (7.40%)	3.0 \pm 0.0	2120.92 \pm 88.18 (87.19%)	2432.52 \pm 137.33		
	Ablation 1	-	96.60 \pm 16.39	1	6.12 \pm 0.70	40.0 \pm 0.0	178.12 \pm 8.39 (6.30%)	3.0 \pm 0.0	2545.16 \pm 710.06 (90.06%)	2826.00 \pm 702.45		
	Ablation 2	-	69.90 \pm 5.21	1	5.48 \pm 0.56	40.0 \pm 0.0	147.90 \pm 14.77 (5.92%)	3.0 \pm 0.0	2277.00 \pm 154.01 (91.07%)	2500.28 \pm 165.34		

TABLE VI: Results of VLM-CAD and both ablation studies. **Red** and **blue** fonts denote the best and second-best UC, respectively.

(a) Results for the amplifier with a complementary input and a class-AB output stage.

PTM	Run	Gain (≥ 65 dB)	UGBW (≥ 10 MHz)	PM ($\geq 50^\circ$)	THD (≤ -26 dB)	Offset (≤ 1 mV)	Power (≤ 10 mW)	UC
180nm	VLM-CAD	85.505	35.111	51.897	-94.375	0.551	0.810	0.081
	Ablation 1	67.447	73.455	111.363	-80.279	0.138	3.120	0.312
	Ablation 2	90.765	13.447	52.568	-139.373	0.018	3.176	0.318
90nm	VLM-CAD	71.808	32.183	52.374	-95.270	0.997	0.366	0.037
	Ablation 1	74.210	62.115	67.292	-68.112	0.591	1.588	0.232
	Ablation 2	94.623	73.014	62.141	-92.835	0.789	1.785	0.179

(b) Results for the two-stage Miller operational amplifier.

PTM	Run	Gain (≥ 54 dB)	UGBW (≥ 1 MHz)	PM ($\geq 60^\circ$)	THD (≤ -60 dB)	Offset (≤ 5 mV)	Power (45-85 μ W)	UC
45nm	VLM-CAD	53.180	1.523	48.703	-77.933	3.838	68.321	2.754
	Ablation 1	45.491	5.960	179.214	-76.714	3.529	111.095	9.816
	Ablation 2	52.783	10.538	17.477	-76.923	2.524	115.607	6.829

guage model agents. The amplifier with a complementary input and a class-AB output stage offers a broad feasible region. However, the two-stage Miller operational amplifier using the 45nm PTM presents a challenge due to manifold sparsity. The combination of high gain and strict power constraints creates a disconnected, needle-in-a-haystack solution space.

This failure underscores a mismatch between model predictions and physical reality: Researchers train language models on general analog circuit corpora that focus on long-channel behavior. However, in the 45nm PTMs, short-channel effects, such as velocity saturation, make standard heuristic sizing rules ineffective. Consequently, the initial designer agent provides seeds that are topologically correct but physically suboptimal, trapping the local optimizer in poor local minima. This situation indicates that future work must incorporate technology-specific adjustments to bridge the gap between general analog circuit theory and the practical realities of nanometer-scale design.

We also present a case of the final design report in Fig 3. The report includes both Global Sensitivity and Elite Sensitivity analyses from ExTuRBO, along with explanations from the Equipped Sizer. By offering quantified sensitivity to the language model, we significantly reduce the risk of generating incorrect explanations.

C. Ablation Study

To demonstrate the significance of circuit schematics and the assistance of Image2Net in helping VLM interpret them, we conduct ablation studies in two distinct paradigms using Gemini 3 Flash Preview: 1) Input only original circuit schematic, with no annotated schematic and JSON description. 2) Input no circuit schematic information at all.

We present all results from our ablation study along with runtime in TABLE V-VI. Our observations indicate that both ablation paradigms for the amplifier with a complementary input and a class-AB output stage meet all specification

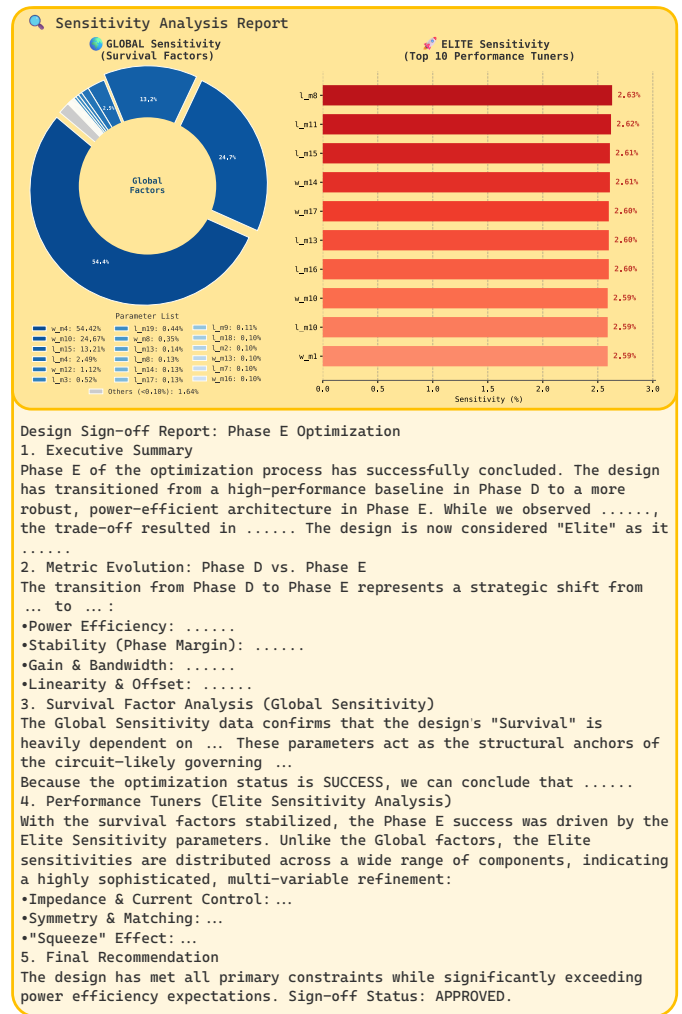


Fig. 3: Final design report including Global Sensitivity, Elite Sensitivity, and corresponding explanations.

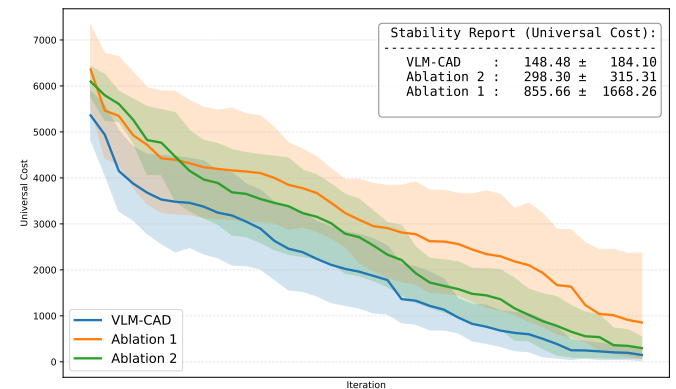


Fig. 4: Universal cost distribution of Phase D for the two-stage Miller operational amplifier, organized from highest to lowest costs. Universal costs of both ablation studies are considerably higher and more unstable than those of VLM-CAD, and ablation 1 performs worse than ablation 2.

requirements, demonstrating the robustness of VLM-CAD. However, ablation studies on both circuits require significantly longer runtimes than VLM-CAD. Specifically, Phase E of both ablation studies accounts for a larger portion of the total runtime than VLM-CAD's. We believe this is due to additional information from Image2Net's thorough schematic interpretation of components and their connections, which supports better analysis in Phase B and consequently provides better seeds for Phase E to optimize.

Additionally, we observe that ablation 1 performs worse and takes a longer time on average than ablation 2. We further reorganize the universal costs for each iteration in Phase D of the two-stage Miller operational amplifier, ranking them from high to low. We visualize the results in Fig. 4 and calculate their average and standard deviation. We find that the universal costs of both ablation studies are considerably higher and more unstable than those of VLM-CAD, further emphasizing the importance of Image2Net for interpreting schematics. Moreover, ablation 1 performs worse than ablation 2. This discrepancy arises since ablation 1 relies solely on the original schematic input. Given that VLM struggles to interpret circuit schematics, this input effectively acts as an adversarial image. Consequently, under visual adversarial attacks, the VLM generates worse seeds than in ablation 2 [23], leading to longer optimization times during Phase E.

V. CONCLUSION

We propose VLM-CAD, a VLM-optimized collaborative agent design workflow. By leveraging Image2Net to aid VLM in interpreting circuit schematics and ExTuRBO for explainable, warm-started optimization, VLM-CAD effectively reduces the risks of hallucination and the lack of transparency that are often seen in existing approaches. Experiment results across multiple PTMs demonstrate VLM-CAD's robustness in satisfying stringent specifications while maintaining low power consumption across two amplifiers, with total runtime under 66 minutes across all experiments. The final design reports, including a quantified sensitivity analysis, effectively bridge the gap between automated optimization and designer trust, marking a step toward reliable agentic automatic analog circuit sizing.

REFERENCES

- [1] A. Girardi, T. De-Oliveira, S. Ghissoni, P. C. Aguirre, and L. Compassi-Severo, "A comprehensive review on automation-based sizing techniques for analog IC design," *J. Integr. Circuits Syst.*, vol. 17, no. 3, pp. 1–14, 2022.
- [2] Z. Wu, Z. Chen, N. Achebe, V. V. Rao, P. Shrestha, and I. Savidis, "Emerging ML-AI Techniques for Analog and RF EDA," *arXiv:2506.00007*, 2025, pp. 9.
- [3] K. G. Liakos and F. Plessas, "Analog Design and Machine Learning: A Review," *Electronics*, vol. 14, no. 17, p. 3541, 2025.
- [4] M. T. M. Emmerich, K. C. Giannakoglou, and B. Naujoks, "Single- and multiobjective evolutionary optimization assisted by Gaussian random field metamodels," *IEEE Trans. Evol. Comput.*, vol. 10, no. 4, pp. 421–439, 2006.
- [5] K. Touloupas and P. P. Sotiriadis, "LoCoMOBO: A Local Constrained Multiobjective Bayesian Optimization for Analog Circuit Sizing," *IEEE Trans. Comput.-Aided Design Integr. Circuits Syst.*, vol. 41, no. 9, pp. 2780–2793, 2022.
- [6] K. Settaluri, A. Haj-Ali, Q. Huang, K. Hakhamaneshi, and B. Nikolic, "AutoCkt: Deep Reinforcement Learning of Analog Circuit Designs," in *2020 Design, Automation & Test in Europe Conference & Exhibition (DATE)*, 2020, pp. 490–495.
- [7] D. V. Kocher, H. Wang, A. P. Chandrakasan, and X. Zhang, "LEDRO: LLM-Enhanced Design Space Reduction and Optimization for Analog Circuits," in *Proc. IEEE Int. Conf. LLM-Aided Design (ICLAD)*, 2025, pp. 141–148.
- [8] S. Xu, H. Zhi, J. Li, and W. Shan, "LLMACD: An LLM-Based Analog Circuit Designer Driven by Behavior Parameters," in *2025 International Symposium of Electronics Design Automation (ISED)*, 2025, pp. 157–162.
- [9] C. Liu, W. Chen, A. Peng, Y. Du, L. Du, and J. Yang, "AmpAgent: An LLM-based Multi-Agent System for Multi-stage Amplifier Schematic Design from Literature for Process and Performance Porting," *arXiv:2409.14739*, 2024.
- [10] M. Ahmadzadeh, K. Chen, and G. Gielen, "(Invited Paper) AnaFlow: Agentic LLM-based Workflow for Reasoning-Driven Explainable and Sample-Efficient Analog Circuit Sizing," in *ICCAD*, 2025, pp. 1–7.
- [11] H.-Y. Hsu and M. P.-H. Lin, "Automatic Analog Schematic Diagram Generation based on Building Block Classification and Reinforcement Learning," in *Proceedings of the 2022 ACM/IEEE Workshop on Machine Learning for CAD*, Virtual Event, China, 2022, pp. 43–48.
- [12] Y. Bang, Z. Ji, A. Schelten, A. Hartshorn, T. Fowler, C. Zhang, N. Cancedda, and P. Fung, "HalluLens: LLM Hallucination Benchmark," *arXiv:2504.17550*, 2025.
- [13] Y. Cao, *Predictive Technology Model for Robust Nanoelectronic Design*, 1st ed. New York, NY: Springer, 2011, pp. XV–173.
- [14] L. Skelic, Y. Xu, M. Cox, W. Lu, T. Yu, and R. Han, "CIRCUIT: A Benchmark for Circuit Interpretation and Reasoning Capabilities of LLMs," *arXiv:2502.07980*, 2025.
- [15] I. Terpstra, "Empowering Analog Integrated Circuit Design through Large Language Models and Reinforcement Learning," M.Eng. thesis, Dept. Elect. Eng. Comput. Sci., Massachusetts Institute of Technology, Cambridge, MA, USA, 2024.
- [16] E. Zhu, Y. Liu, Z. Zhang, X. Li, J. Zhou, X. Yu, M. Huang, and H. Wang, "MAPS: Advancing Multi-Modal Reasoning in Expert-Level Physical Science," in *Proc. Int. Conf. Learn. Represent.*, 2025.
- [17] Z. Zhao, A. Daiv, and D. Porras, "CURVLM: Circuit Understanding Via Group Relative Policy Optimization (GRPO) on Vision Language Models," *CS231n: Deep Learning for Computer Vision*, Stanford, Final Project Reports, Highlight, Spring 2025.
- [18] P. Rahmazadehgervi, L. Bolton, M. R. Taesiri, and A. T. Nguyen, "Vision language models are blind," in *Proc. Asian Conf. Computer Vision (ACCV)*, Dec. 2024, pp. 18–34.
- [19] B. Razavi, "Analog Design Experiments With AI—Part 1 [The Analog Mind]," *IEEE Solid-State Circuits Mag.*, vol. 17, no. 4, pp. 11–15, 2025.
- [20] C. Liu and D. Chitnis, "EEsizer: LLM-Based AI Agent for Sizing of Analog and Mixed Signal Circuit," *IEEE Trans. Circuits Syst. I, Reg. Papers*, pp. 1–10, 2025.
- [21] M. Ahmadzadeh, J. Lappas, N. Wehn, and G. Gielen, "AnaCraft: Duel-Play Probabilistic-Model-based Reinforcement Learning for Sample-Efficient PVT-Robust Analog Circuit Sizing Optimization," *IEEE Trans. Comput.-Aided Des. Integr. Circuits Syst.*, early access, 2025.
- [22] A. Yang et al., "Qwen3 Technical Report," *arXiv* preprint *arXiv:2505.09388*, 2025.
- [23] X. Cui, A. Aparcedo, Y. K. Jang, and S.-N. Lim, "On the Robustness of Large Multimodal Models Against Image Adversarial Attacks," in *Proc. IEEE/CVF Conf. Comput. Vis. Pattern Recognit. (CVPR)*, June 2024, pp. 24625–24634.